

**Two-dimensional
performance of
MIPAS observation
modes**

M. Carlotti et al.

Two-dimensional performance of MIPAS observation modes in the upper-troposphere/lower-stratosphere

M. Carlotti¹, E. Papandrea¹, and E. Castellì^{2,3}

¹Dipartimento di Chimica Fisica e Inorganica, University of Bologna, Viale Risorgimento 4, 40136 Bologna, Italy

²Istituto di Scienze dell'Atmosfera e del Clima, CNR, Via P. Gobetti 101, 40129 Bologna, Italy

³Istituto per le Applicazioni del Calcolo "Mauro Picone", CNR, Via Madonna del Piano 10, 50019 Sesto Fiorentino (FI), Italy

Received: 25 May 2010 – Accepted: 28 June 2010 – Published: 8 July 2010

Correspondence to: M. Carlotti (carlotti@fci.unibo.it)

Published by Copernicus Publications on behalf of the European Geosciences Union.

This discussion paper is/has been under review for the journal Atmospheric Measurement Techniques (AMT). Please refer to the corresponding final paper in AMT if available.

Title Page

Abstract

Introduction

Conclusions

References

Tables

Figures

⏪

⏩

◀

▶

Back

Close

Full Screen / Esc

Printer-friendly Version

Interactive Discussion

Abstract

In this paper we analyze the performance of the three MIPAS (Michelson Interferometer for Passive Atmospheric Sounding) observation modes that sound the Upper-Troposphere/Lower-Stratosphere (UT/LS) region. The two-dimensional (2-D) tomographic retrieval approach is assumed to derive the atmospheric field of geophysical parameters. For each observation mode we have calculated the 2-D distribution of the *information load* quantifier relative to the main MIPAS targets. The performance of the observation modes is then evaluated in terms of strength, spatial coverage and uniformity of the information-load distribution along the full orbit. The outcome of the information-load analysis has been validated with simulated retrievals based on the observational parameters of real orbits. With this strategy we have assessed the precision and the spatial (both horizontal and vertical) resolution of the retrieval products. The performance of the three observation modes has been compared for the MIPAS main products in both the UT/LS and the extended altitude range. This study shows that the two observation modes that were specifically designed for the UT/LS region are actually competitive with the third one, designed for the whole stratosphere, up to altitudes that far exceed the UT/LS. In the UT/LS the performance of the two specific observation modes is comparable even if the best performance in terms of horizontal resolution is provided by the observation mode that was excluded by the European Space Agency (ESA) from the current MIPAS duty cycle. This paper reports the first application of the information-load analysis and highlights the validity of this approach.

1 Introduction

The Michelson Interferometer for Passive Atmospheric Sounding (MIPAS) in its present configuration can measure the atmosphere with seven different observation modes. Two of them have been expressly designed to sound the Upper-Troposphere/Lower-Stratosphere (UT/LS) region although one of them has been operated for only 36 test

AMTD

3, 2861–2890, 2010

Two-dimensional performance of MIPAS observation modes

M. Carlotti et al.

Title Page

Abstract

Introduction

Conclusions

References

Tables

Figures

⏪

⏩

◀

▶

Back

Close

Full Screen / Esc

Printer-friendly Version

Interactive Discussion



Two-dimensional performance of MIPAS observation modesM. Carlotti et al.

[Title Page](#)[Abstract](#)[Introduction](#)[Conclusions](#)[References](#)[Tables](#)[Figures](#)[⏪](#)[⏩](#)[◀](#)[▶](#)[Back](#)[Close](#)[Full Screen / Esc](#)[Printer-friendly Version](#)[Interactive Discussion](#)

in the horizontal domain. The limb-scanning pattern of NOM consists of 27 observation geometries. Starting from the bottom the first 11 tangent altitudes of NOM are separated by 1.5 km; altitude steps of 2, 3, and 4 km space out the next groups of 5, 5, and 6 tangent altitudes respectively. This limb pattern, combined with the ENVISAT orbit period of 101 min, generates about 96 limb-scans per orbit with an average separation of about 415 km between consecutive limb-scans. For UTLS-1 the limb-scanning pattern consists of 19 observation geometries; the first 9 tangent altitudes are separated by 1.5 km; 2, 3, 4, and 4.5 km space out the next groups of 3, 2, and 4 tangent altitudes respectively. This limb pattern generates about 125 limb-scans per orbit separated by about 320 km. For NOM and UTLS-1 the limb-scanning patterns are shifted in altitude along the orbit following a model that imitates the varying altitude of the tropopause as a function of latitude. Finally, in UTLS-2 the limb-scanning pattern consists of 11 observation geometries; tangent altitudes are separated by 2 km from 12 to 20 km, 3 and 4 km space out the next two groups of three tangent altitudes up to a maximum of 42 km. This pattern generates about 213 limb-scans per orbit separated by about 190 km. The UTLS-2 has been operated for a very limited number of orbits (36). The three panels of Fig. 1 show the layout of MIPAS tangent points along orbits measured with NOM (top), UTLS-1 (middle) and UTLS-2 (bottom) respectively. In Fig. 1 the altitude of tangent points is plotted as a function of the Orbital Coordinate (OC) defined as the polar angle originating at the North Pole and spanning the orbit plane over its 360 deg extension. We can appreciate in Fig. 1 few minor gaps that occur in the horizontal sampling of the atmosphere of the three observation modes. Besides, the UTLS-1 shows a major gap that is present (even if at different positions) in all the orbits recorded with this observation mode. A detailed discussion of the MIPAS experiment can be found in Fisher et al. (2008).

3 Mathematical tools

3.1 Retrieval strategy

MIPAS spectra are analyzed by the ESA ground processor that determines, at the tangent points of each limb scan, the values of pressure, temperature and Volume Mixing Ratio (VMR) of six key atmospheric species (H_2O , O_3 , HNO_3 , CH_4 , N_2O and NO_2). For this purpose ESA employs a 1-D retrieval system (Ridolfi et al., 2000) that implements the global-fit algorithm (Carlotti, 1988). A 2-D algorithm, named Geo-fit (Carlotti et al., 2001), was subsequently developed for the analysis of MIPAS measurements and implemented in the operational code GMTR (Carlotti et al., 2006); the study reported in this paper refers to this kind of retrieval. The Geo-fit approach is based on the simultaneous inversion of observations selected from all the limb scans measured along a whole orbit. This strategy permits to merge the information on each retrieval parameter from different observation geometries and makes it possible to model the horizontal variability of the atmosphere. In a Geo-fit the 2-D retrieval grid is fully independent from the measurement grid (i.e. the grid identified by the tangent points of the measurements). By exploiting this feature atmospheric profiles can be retrieved with horizontal separations that are different from those of the measured limb scans. Nevertheless, adopting the assumption that the information is mostly concentrated around the tangent point of the observations, the straightforward choice is a horizontal retrieval grid defined by the average geographical coordinates of the tangent points of the limb-scans. We will denote this choice as “natural” grid.

Irrespective of the specific retrieval algorithm, MIPAS observations are analyzed using a non-linear least squares fit based on the Gauss-Newton method (Ridolfi et al., 2000; Carlotti et al., 2006). The general iterative solution expression:

$$\Delta \mathbf{x} = (\mathbf{x}_{i+1} - \mathbf{x}_i) = [\mathbf{K}^T \mathbf{S}_n^{-1} \mathbf{K} + \lambda \mathbf{I} + \mathbf{R}]^{-1} [\mathbf{K}^T \mathbf{S}_n^{-1} \mathbf{n} - \mathbf{R}(\mathbf{x}_i - \mathbf{x}_a)] \quad (1)$$

is used to compute, at iteration $i + 1$, the correction $\Delta \mathbf{x}$ to the state vector \mathbf{x}_i . The state vector includes the values of the target quantities at all the geo-located retrieval grid

Two-dimensional performance of MIPAS observation modes

M. Carlotti et al.

Title Page

Abstract

Introduction

Conclusions

References

Tables

Figures

⏪

⏩

◀

▶

Back

Close

Full Screen / Esc

Printer-friendly Version

Interactive Discussion



associated with parameter k is the vector $\mathbf{a}(k, j)$, $j = 1 \dots p$ (where p is the number of individual grid points) that corresponds to the k -th row of matrix \mathbf{A} . The vertical resolution of a retrieval parameter is defined as the FWHM of the bell-shaped feature identified by the subset of elements of vector \mathbf{a} that correspond to the value θ_k of the OC. In a similar way the horizontal resolution is defined as the FWHM of the subset of elements of \mathbf{a} that correspond to the altitude z_k .

3.3 Information load

In a 2-D approach it is possible to associate to each element of the atmospheric discretization a quantifier that measures the amount of information carried by that element with respect to a retrieval target (Carlotti and Magnani, 2009). The discretization of the atmosphere is operated on both the vertical and the horizontal domains (Carlotti et al., 2001). In the vertical domain altitude levels delimit layers as in a 1-D approach. The horizontal discretization is built using segments perpendicular to the Earth's geoid (radii) and extended up to the boundary of the atmosphere. The 2-D discretization leads to a web-like picture in which consecutive levels and radii define plane figures that are denoted as "cloves". It is then possible to assign to each clove h the Ω quantifier defined as (Carlotti and Magnani, 2009):

$$\Omega(q, h) = \left[\sum_{i=1}^l \sum_{j=1}^m \sum_{k=1}^n \left(\frac{\partial S_{ijk}}{\partial q_h} \right)^2 \right]^{1/2} \quad (4)$$

where:

$\Omega(q, h)$ = information load of clove h with respect to atmospheric parameter q ,
 S_{ijk} = spectral signal of observation geometry i at frequency j of the analyzed MW k ,
 l = number of observation geometries that go through clove h ,
 m = number of analyzed MWs in observation geometry i ,
 n = number of spectral points in MW j .

Two-dimensional performance of MIPAS observation modes

M. Carlotti et al.

Title Page

Abstract

Introduction

Conclusions

References

Tables

Figures

⏪

⏩

◀

▶

Back

Close

Full Screen / Esc

Printer-friendly Version

Interactive Discussion



The column vector containing the set of elements within the triple summation in Eq. (4) is the Jacobian matrix (see Eq. 1) corresponding to the retrieval of target parameter q in clove h . If we assume that the observations are uncorrelated and characterized by constant uncertainty ($\mathbf{S}_n = \mathbf{I}$) and we neglect external constraints, the term in square brackets of Eq. (2) turns into:

$$(\mathbf{K}^T \mathbf{K})_h = \sum_{i=1}^l \sum_{j=1}^m \sum_{k=1}^n \left(\frac{\partial S_{ijk}}{\partial q_h} \right)^2 \quad (5)$$

Therefore, in a retrieval analysis the uncertainty on the value of the target quantity q in clove h would be given by $1/\Omega$ (see Eq. 2). The value of Ω can be calculated for each clove of the 2-D discretization so that, for each retrieval target, we can draw a map of the 2-D distribution of the Ω quantifier.

4 Information-load analysis

We have calculated 2-D maps of Ω for complete orbits operated with NOM, UTLS-1 and UTLS-2. Maps relative to all MIPAS main targets (see Sect. 3.1) have been compared in terms of intensity, altitude coverage and uniformity of the Ω distribution. As an example, Fig. 2 shows, the distribution of Ω with respect to the temperature along an orbit measured with the NOM observation mode. For the calculation of Ω we used atmospheric fields corresponding to climatological profiles, taken from Remedios et al. (2007), relative to a January atmosphere. The MWs are those selected for the MIPAS operational retrievals. In Fig. 2 the vertical dimension of the atmosphere is expanded by a factor of 30 (for the sake of clarity) with respect to the extension of the Earth's radius. Values of the orbital coordinate are reported in Fig. 2 for convenience. The Ω distributions have been calculated for a 2-D discretization of the atmosphere (Carlotti et al., 2001) operated with altitude levels evenly spaced by 1 km and radii evenly spaced by 0.25 latitudinal degrees (about 28 km). A comparison of Ω for temperature in the three observation modes is shown in the panels of Fig. 3 that reports

Two-dimensional performance of MIPAS observation modes

M. Carlotti et al.

Title Page

Abstract

Introduction

Conclusions

References

Tables

Figures

⏪

⏩

◀

▶

Back

Close

Full Screen / Esc

Printer-friendly Version

Interactive Discussion



targets the Ω differences inspection indicates that, in the lower stratosphere, the Ω distribution for UTLS-2 observations is comparable and sometimes better than that for the UTLS-1 observations.

The information-load analysis on the eight MIPAS main targets indicates that:

1. the performance of the two UT/LS modes is competitive with that of the NOM mode even in altitude ranges that exceed the UT/LS region,
2. in the UT/LS some of the UTLS-2 products should be of better quality than the corresponding UTLS-1 products.

5 Simulated retrievals

The results of the information-load analysis can be verified by investigating retrievals performed for simulated observations. The steps of this kind of retrieval are:

1. generate simulated observations with a standalone forward model; reference altitude profiles are used for the target quantity in this step. The observational parameters are taken from a real MIPAS orbit,
2. perform the retrieval analysis on the simulated observations using an initial guess obtained by applying random perturbations to the reference profiles,
3. evaluate the retrieval precision by comparing the retrieved values with the reference values used to generate the simulated observations,
4. evaluate the horizontal and the vertical resolution of the retrieval products by means of the 2-D averaging kernels (Rodgers, 2000).

For all the tests reported in this section the maximum allowed perturbations applied in step 2 were 5%, 1%, and 50% for pressure, temperature, and VMR profiles respectively. Maximum perturbations of 80% were applied to atmospheric continuum profiles which, to simulate real retrievals, are also included in the state vector \mathbf{x}_i of Eq. (1).

Two-dimensional performance of MIPAS observation modes

M. Carlotti et al.

Title Page

Abstract

Introduction

Conclusions

References

Tables

Figures



Back

Close

Full Screen / Esc

Printer-friendly Version

Interactive Discussion



5.1 Performance on the NOM retrieval grid

In order to verify whether the two UT/LS modes are competitive with NOM at altitudes that exceed the UT/LS region we have evaluated the performance of the three modes in the retrieval conditions that are operationally used for the NOM. A common retrieval grid has been used with altitude steps defined by the geometrical separation between the NOM observation geometries (with the exception for the lower limit of 12 km adopted for UTLS-2 due to its limb-scanning pattern (see Fig. 1)); in the horizontal domain 96 profiles were retrieved at the NOM natural grid (see Sects. 2 and 3.1). Common MWs and auxiliary data (those adopted for the NOM operational analyses) have been used in the simulated retrievals reported in this and in the next sub-section. No constraints to the solution were imposed for the main targets in all the simulated retrievals presented in this paper ($\mathbf{R} = \mathbf{0}$ in Eq. (1)). Weak a-priori information was adopted in order to stabilize the retrieval of atmospheric continuum parameters.

An example of the results of a simulated retrieval is given in Fig. 5 which refers to N_2O VMR retrieved from UTLS-2 observations (since the behaviour of N_2O is quite representative we will use this target also for the following examples). Panel (a) of Fig. 5 shows the retrieved VMRs, panel (b) the absolute value of the difference between retrieved and reference VMRs, panels (c) and (d) the vertical and the horizontal resolution of the retrieval products respectively. In panel (d) of Fig. 5 are present vertical stripes that correspond to the wider separations between the limb-scans (see Sect. 2). Figure 5 shows that N_2O can be retrieved from UTLS-2 with acceptable precision well above the highest tangent altitude of the observations. Above this altitude the vertical resolution increases as expected while the horizontal resolution seems to improve. However, at higher altitudes the information load decreases due to the decreasing N_2O VMR (see panel (a)); in these conditions the subset of elements of vector \mathbf{a} of the averaging kernel depicts a distorted feature that is no longer bell-shaped as required by the definition of spatial resolution given in Sect. 3.2. Such a situation is generally encountered where the information load is weak and/or irregularly scattered.

Two-dimensional performance of MIPAS observation modes

M. Carlotti et al.

Title Page

Abstract

Introduction

Conclusions

References

Tables

Figures

⏪

⏩

◀

▶

Back

Close

Full Screen / Esc

Printer-friendly Version

Interactive Discussion



10 km (lower limit of UTLS-2 observations) and below about 40 km (where the spatial resolution of this observation mode cannot be evaluated).

The overall results of the above comparison performed on the NOM retrieval grid support the reliability of the information-load analysis that indicates (see Sect. 3) a competitive performance of the two UT/LS observation modes at altitudes that exceed the UT/LS region.

5.2 Performance in the UT/LS

Focusing on the UT/LS region (below 25 km) we first investigate the performance of each observation mode when its natural grid (see Sect. 3.1) is used in the horizontal domain for the retrievals. In the vertical domain the profiles are defined at the same altitudes as in Sect. 5.1 up to 25 km and, above, at the tangent altitudes of the specific observation mode. The natural grids have (in accordance with the observational parameters given in Sect. 2): 96 profiles separated by about 415 km for NOM, 125 profiles separated by about 320 km for UTLS-1, and 213 profiles separated by about 190 km for UTLS-2 retrievals.

In order to assess the appropriateness of the natural retrieval grids we have investigated the behaviour of the horizontal resolution of the retrieval products obtained on these grids. The left panel of Fig. 7 shows, for an OC interval of 50 deg, the horizontal resolution of N_2O VMRs when retrieved from UTLS-2 observations using its natural retrieval grid. The colours alternation that appears in this map along the OC indicates that the resolution requirements of the UTLS-2 natural grid trigger a retrieval instability due to an insufficient information load of the observations. The observed oscillation can be reduced by increasing the horizontal separation of the profiles (Carlotti et al., 2007) (we have observed in Sect. 4 that in the case of UTLS-2 the retrieval grid can be defined arbitrary because of the uniform Ω distributions that it generates). Following this strategy we have found that a separation of 2.25 deg (160 profiles separated by about 250 km) leads to a satisfactory stability of the UTLS-2 retrievals. An example of the improvement is given in the right panel of Fig. 7 that shows, at 18 km, the horizontal

Two-dimensional performance of MIPAS observation modes

M. Carlotti et al.

Title Page

Abstract

Introduction

Conclusions

References

Tables

Figures

⏪

⏩

◀

▶

Back

Close

Full Screen / Esc

Printer-friendly Version

Interactive Discussion



resolution extracted from the map in the left panel (green line) and the horizontal resolution when the 2.25 deg separation is used for the horizontal grid (red line).

As for the performance of UTLS-1 Fig. 8 shows, in its left panel, the horizontal resolution of N₂O VMRs when retrieved from UTLS-1 observations using their natural grid.

It can be seen in Fig. 8 that the retrieval is rather stable then indicating that the geometrical separations of the UTLS-1 natural grid are consistent with the information load of the observations.

In a further step we have explored the possibility to improve the horizontal resolution of the UTLS-1 products by reducing the geometrical steps in the horizontal retrieval grid. We have found that even moderate reductions of the horizontal step trigger instabilities that, as in the UTLS-2 case, appear as oscillations. As an example we show in the right hand panel of Fig. 8 the values of the horizontal resolution at 18 km extracted from the map in the left hand panel (green line) and the values, at the same altitude, when the 2.25 deg separation is used for the horizontal grid (red line).

The behaviour of the vertical resolution reflects the one of 1-D retrievals when the horizontal grid does not trigger the instabilities discussed in the previous paragraph. Oscillations appear also in the vertical domain when the horizontal resolution becomes markedly unstable.

The analysis that we have shown for N₂O is basically representative of the behaviour of the other main MIPAS targets with the exception of NO₂ that, in the case of UTLS-2 suffers from instabilities in the vertical domain. However, considering that NO₂ is of minor importance at those altitudes, we can state that in the UT/LS the natural grid is suitable for the retrievals on UTLS-1 observations while the 2.25 deg grid provides a satisfactory trade-off in the case of UTLS-2 observations. The performance obtained using these grids is shown in Fig. 9 that reports the same quantifiers (and with the same formats) as in Fig. 6. In Fig. 9 the plots relative to NOM are also included for reference; these plots are just a blow up of the plots in Fig. 6 since they refer to retrievals carried out using (as in Fig. 6) the natural grid of the NOM observation mode. The analysis of Fig. 9 shows that in the UT/LS:

Two-dimensional performance of MIPAS observation modes

M. Carlotti et al.

Title Page

Abstract

Introduction

Conclusions

References

Tables

Figures

⏪

⏩

◀

▶

Back

Close

Full Screen / Esc

Printer-friendly Version

Interactive Discussion



Two-dimensional performance of MIPAS observation modes

M. Carlotti et al.

Title Page

Abstract

Introduction

Conclusions

References

Tables

Figures

⏪

⏩

◀

▶

Back

Close

Full Screen / Esc

Printer-friendly Version

Interactive Discussion

- 5 – in the UT/LS the information-load distributions generated by UTLS-2 show, in general, higher intensities and better uniformity than those generated by UTLS-1. The high uniformity indicates that for the UTLS-2 analyses the retrieval grid can be selected on the basis of only the trade-off between precision and spatial resolution.

In order to validate the outcomes of the information-load analysis and to get quantitative estimates about the performance of the three observation modes, we have carried out simulated retrievals. With this strategy we have evaluated precision and spatial resolution of the MIPAS targets retrieved from each observation mode.

10 The results obtained with the simulated retrievals confirm the indications of the information-load analysis. In particular they have shown that:

- 15 – the quality of the profiles retrieved from the two observation modes that were specifically designed for the UT/LS region is similar to that retrieved from the NOM mode (that was designed for the whole stratosphere) up to altitudes that far exceed the UT/LS,
- in the UT/LS the performance of the two specific observation modes is comparable. In terms of horizontal resolution the best performance is provided by the UTLS-2 mode that was excluded by ESA from the current MIPAS duty cycle.

20 These results have been obtained with the analysis of the MWs used for the MIPAS operational retrievals. Different MWs could be selected in order to enhance the performance of a specific observation mode in the altitude range of interest. In this task of selection the performance of different sets of MWs can be tested with the information-load analysis that, as we have shown in this study, has proven to be a reliable tool.

25 *Acknowledgements.* E. Papandrea acknowledges support by ESA within the framework of the Changing Earth Science Network Initiative.

References

- Carlotti, M.: Global-Fit Approach to the Analysis of Limb-scanning Atmospheric Measurements, *Appl. Optics*, 27, 3250–3254, 1988.
- Carlotti, M., Dinelli, B. M., Raspollini, P., and Ridolfi, M.: Geo-fit approach to the analysis of limb-scanning satellite measurements, *Appl. Optics*, 40, 1872–1885, 2001.
- Carlotti, M., Brizzi, G., Papandrea, E., Prevedelli, M., Ridolfi, M., Dinelli, B. M., and Magnani, L.: GMTR: two-dimensional multi-target retrieval model for MIPAS/ENVISAT observations, *Appl. Optics*, 45, 716–727, 2006.
- Carlotti, M., Dinelli, B. M., Papandrea, E. and Ridolfi, M.: Assessment of the horizontal resolution of retrieval products derived from MIPAS observations, *Opt. Express*, 15, 10458–10472, 2007.
- Carlotti, M. and Magnani, L.: Two-dimensional sensitivity analysis of MIPAS observations, *Opt. Express*, 17, 7, 5340–5357, 2009.
- Dudhia, A., Jay, V. L., and Rodgers, C. D.: Microwindow selection for high-spectral-resolution sounders, *Appl. Optics*, 41, 3665–3673, 2002.
- Fischer, H., Birk, M., Blom, C., Carli, B., Carlotti, M., von Clarmann, T., Delbouille, L., Dudhia, A., Ehhalt, D., Endemann, M., Flaud, J. M., Gessner, R., Kleinert, A., Koopman, R., Langen, J., López-Puertas, M., Mosner, P., Nett, H., Oelhaf, H., Perron, G., Remedios, J., Ridolfi, M., Stiller, G., and Zander, R.: MIPAS: an instrument for atmospheric and climate research, *Atmos. Chem. Phys.*, 8, 2151–2188, doi:10.5194/acp-8-2151-2008, 2008.
- Marquardt, D. W.: An algorithm for the least-squares estimation of non-linear parameters, *SIAM J. Soc. Appl. Math.*, 11, 2, 431–441, 1963.
- Remedios, J. J., Leigh, R. J., Waterfall, A. M., Moore, D. P., Sembhi, H., Parkes, I., Greenhough, J., Chipperfield, M. P., and Hauglustaine, D.: MIPAS reference atmospheres and comparisons to V4.61/V4.62 MIPAS level 2 geophysical data sets, *Atmos. Chem. Phys. Discuss.*, 7, 9973–10017, doi:10.5194/acpd-7-9973-2007, 2007.
- Ridolfi, M., Carli, B., Carlotti, M., von Clarmann, T., Dinelli, B. M., Dudhia, A., Flaud, J. M., Hoepfner, M., Morris, P. E., Raspollini, P., Stiller, G., and Wells, R. J.: Optimized forward model and retrieval scheme for MIPAS near-real-time data processing, *Appl. Optics*, 39, 1323–1340, 2000.
- Rodgers, C. D.: Inverse methods for atmospheric sounding: Theory and Practice, Series on Atmospheric, Oceanic and Planetary Physics, World Scientific Publishing Co., Singapore,

AMTD

3, 2861–2890, 2010

Two-dimensional performance of MIPAS observation modes

M. Carlotti et al.

Title Page

Abstract

Introduction

Conclusions

References

Tables

Figures

⏪

⏩

◀

▶

Back

Close

Full Screen / Esc

Printer-friendly Version

Interactive Discussion

Vol. 2, 65–100, 2000.
Worden, J. R., Bowman, K. W., and Jones, D. B.: Two-dimensional characterization of atmospheric profile retrievals from limb sounding observations, *J. Quant. Spectrosc. Radiat. Transfer*, 86, 45–71, 2004.

Two-dimensional performance of MIPAS observation modes

M. Carlotti et al.

Title Page

Abstract

Introduction

Conclusions

References

Tables

Figures

⏪

⏩

◀

▶

Back

Close

Full Screen / Esc

Printer-friendly Version

Interactive Discussion



Two-dimensional performance of MIPAS observation modes

M. Carlotti et al.

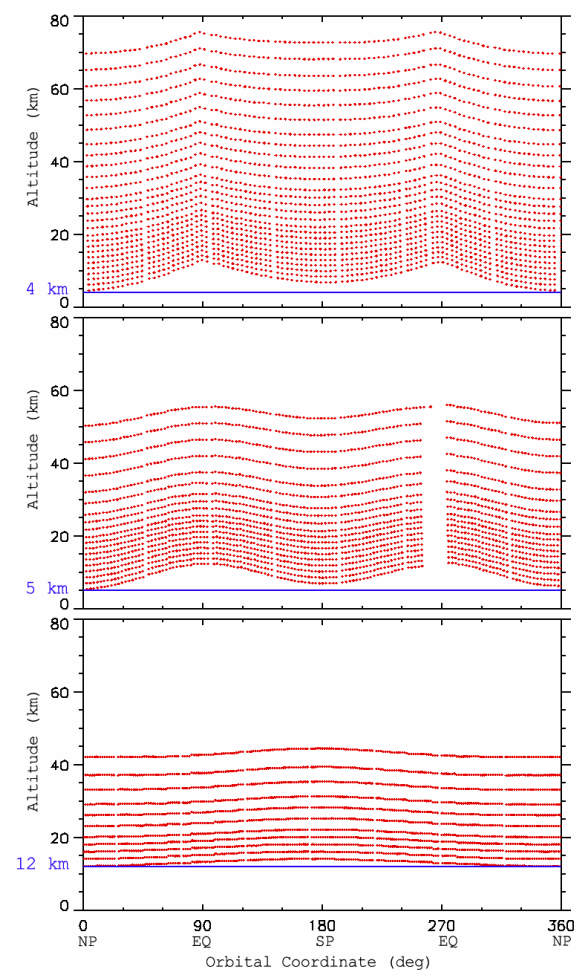


Fig. 1. Tangent points along orbits measured with NOM (top), UTLS-1 (middle) and UTLS-2 (bottom). Earth poles (NP, SP) and Equator (EQ) are marked on the abscissa axis.

Title Page

Abstract Introduction

Conclusions References

Tables Figures

◀ ▶

◀ ▶

Back Close

Full Screen / Esc

Printer-friendly Version

Interactive Discussion



Two-dimensional performance of MIPAS observation modes

M. Carlotti et al.

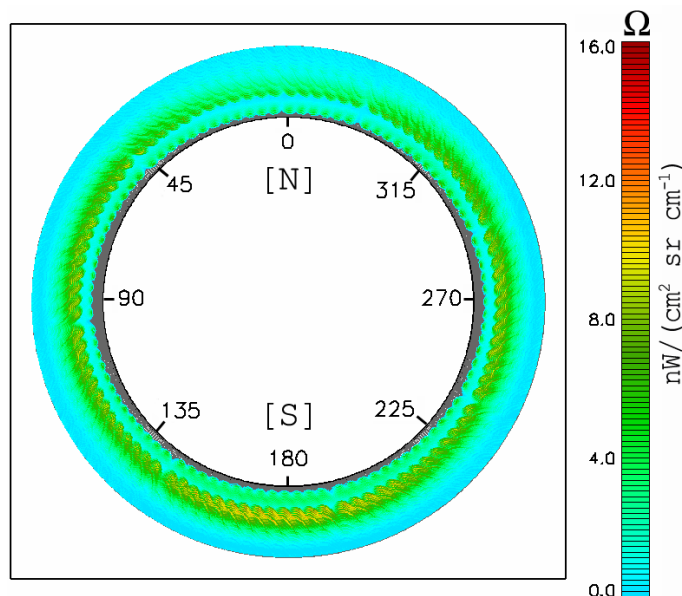


Fig. 2. Distribution of Ω with respect to the temperature along a MIPAS orbit measured with the NOM observation mode. Values of the OC and position of the geographical poles are reported within the figure. The vertical dimension of the atmosphere is expanded by a factor of 30 with respect to the extension of the Earth's radius.

[Title Page](#)
[Abstract](#)
[Introduction](#)
[Conclusions](#)
[References](#)
[Tables](#)
[Figures](#)
[◀](#)
[▶](#)
[◀](#)
[▶](#)
[Back](#)
[Close](#)
[Full Screen / Esc](#)
[Printer-friendly Version](#)
[Interactive Discussion](#)

Two-dimensional performance of MIPAS observation modes

M. Carlotti et al.

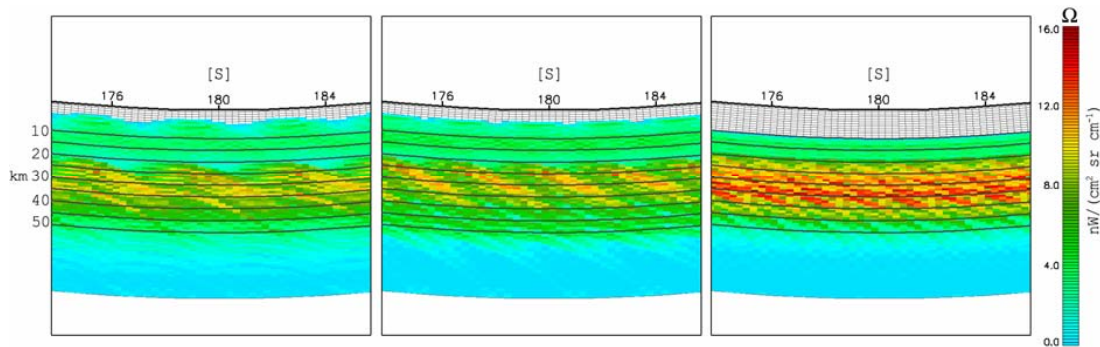


Fig. 3. Blow-up of the Ω distributions with respect to temperature around the South Pole in the case of NOM (left-), UTLS-1 (middle-) and UTLS-2 (right-panel). The vertical dimension of the atmosphere is expanded by a factor of 10 with respect to the extension of the Earth's radius.

[Title Page](#)[Abstract](#)[Introduction](#)[Conclusions](#)[References](#)[Tables](#)[Figures](#)[◀](#)[▶](#)[◀](#)[▶](#)[Back](#)[Close](#)[Full Screen / Esc](#)[Printer-friendly Version](#)[Interactive Discussion](#)

Two-dimensional performance of MIPAS observation modes

M. Carlotti et al.

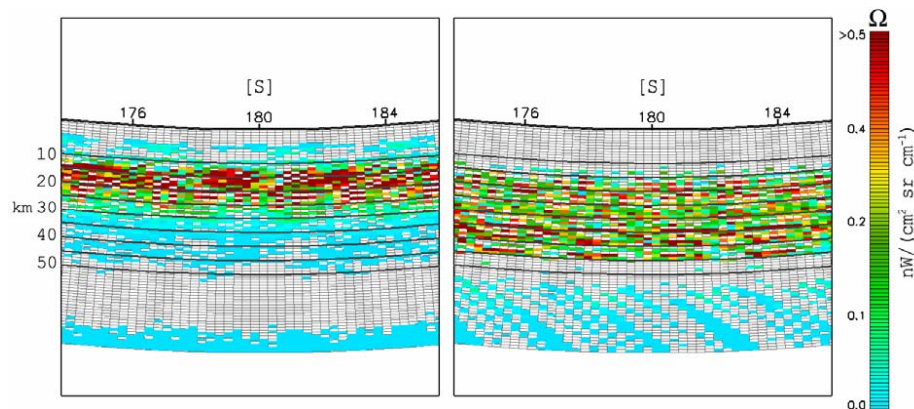


Fig. 4. Left panel: Difference between the Ω distributions generated by UTLS-1 and NOM observation modes for the HNO_3 VMR. Right panel: difference between the Ω distributions generated by UTLS-2 and UTLS-1 in the case of O_3 . The vertical dimension of the atmosphere is expanded by a factor of 10 with respect to the extension of the Earth's radius.

Title Page

Abstract

Introduction

Conclusions

References

Tables

Figures

⏪

⏩

◀

▶

Back

Close

Full Screen / Esc

Printer-friendly Version

Interactive Discussion

Two-dimensional performance of MIPAS observation modes

M. Carlotti et al.

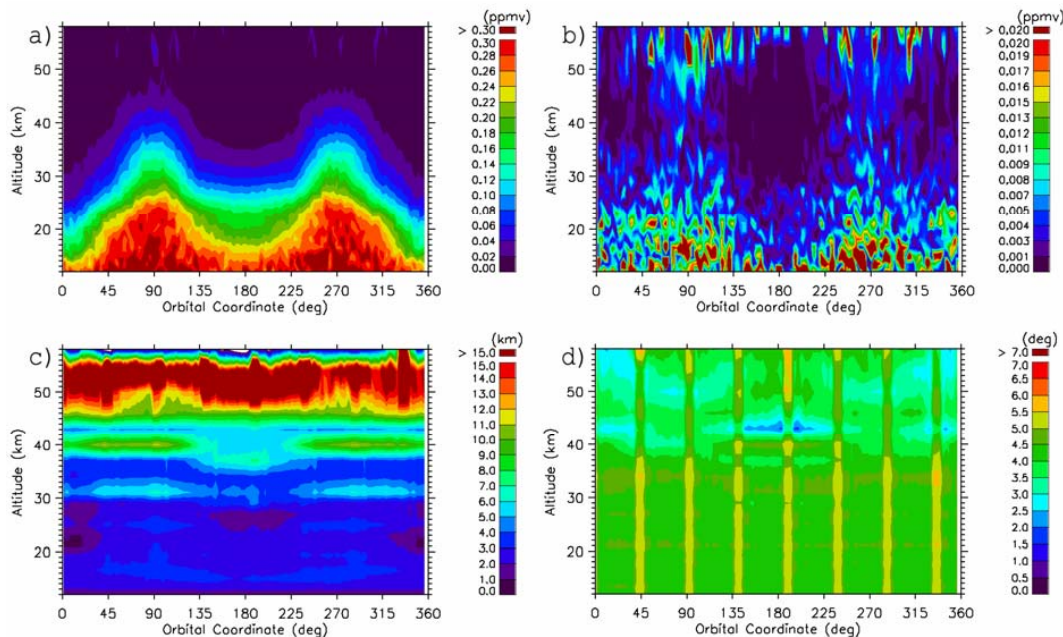


Fig. 5. Results relative to the retrieval of N₂O VMR from UTLIS-2 observations. Panel **(a)** retrieved values, panel **(b)** absolute value of the difference between retrieved and reference VMRs, panel **(c)** vertical resolution, panel **(d)** horizontal resolution.

[Title Page](#)[Abstract](#)[Introduction](#)[Conclusions](#)[References](#)[Tables](#)[Figures](#)[◀](#)[▶](#)[◀](#)[▶](#)[Back](#)[Close](#)[Full Screen / Esc](#)[Printer-friendly Version](#)[Interactive Discussion](#)

Two-dimensional performance of MIPAS observation modes

M. Carlotti et al.

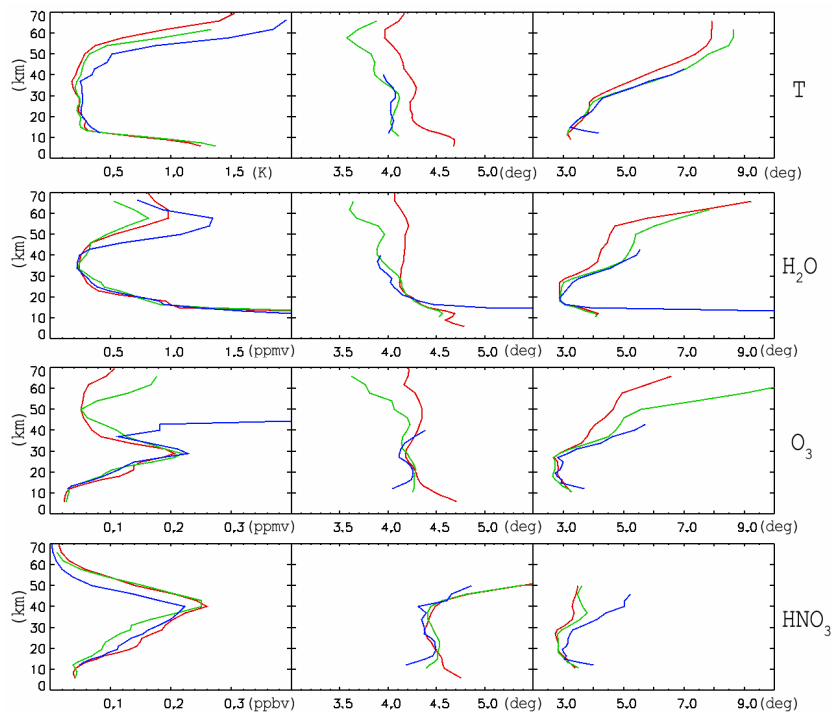


Fig. 6. Standard deviation of the difference between retrieved and the reference profiles (left column), average horizontal resolution (middle column) and average vertical resolution (right column) for NOM (red), UTLS-1 (green) and UTLS-2 (blue). Target is identified on the right side.

**Two-dimensional
performance of
MIPAS observation
modes**

M. Carlotti et al.

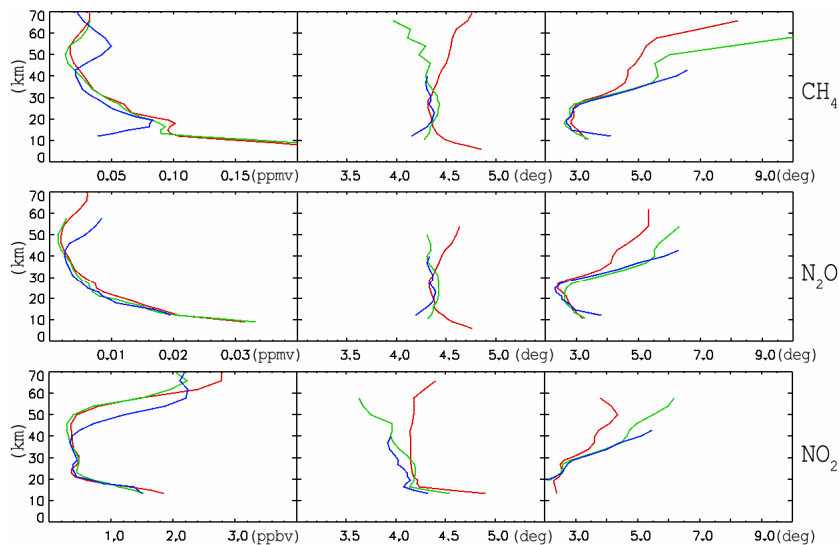


Fig. 6. Continued.

Title Page

Abstract

Introduction

Conclusions

References

Tables

Figures

◀

▶

◀

▶

Back

Close

Full Screen / Esc

Printer-friendly Version

Interactive Discussion

Two-dimensional performance of MIPAS observation modes

M. Carlotti et al.

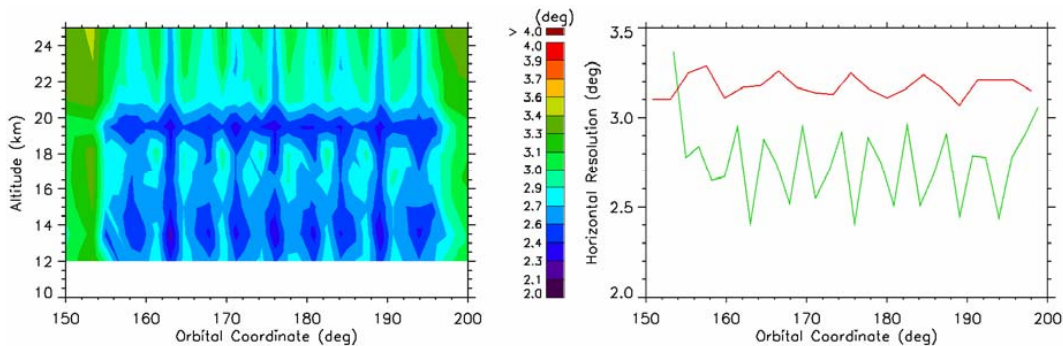


Fig. 7. Left panel: horizontal resolution of N_2O VMRs when retrieved from UTLS-2 observations using the natural retrieval grid. Right panel: values of the horizontal resolution at 18 km extracted from the map in the left panel (green line) and values, at the same altitude, when the 2.25 deg separation is used for the horizontal grid (red line).

[Title Page](#)[Abstract](#)[Introduction](#)[Conclusions](#)[References](#)[Tables](#)[Figures](#)[⏪](#)[⏩](#)[◀](#)[▶](#)[Back](#)[Close](#)[Full Screen / Esc](#)[Printer-friendly Version](#)[Interactive Discussion](#)

Two-dimensional performance of MIPAS observation modes

M. Carlotti et al.

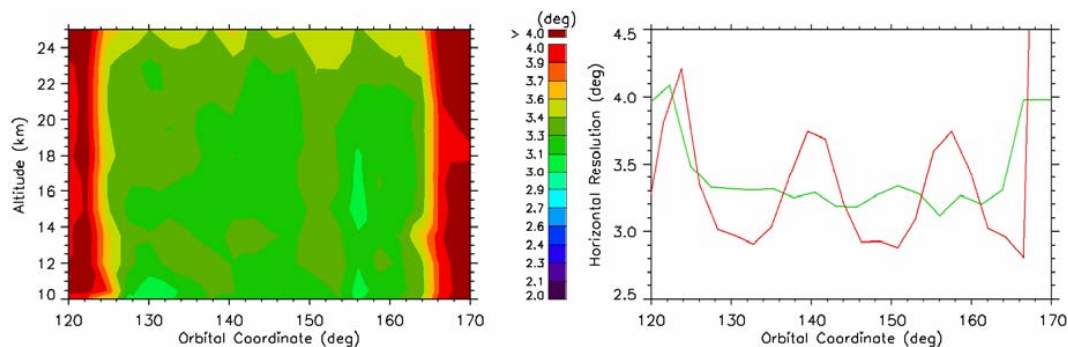


Fig. 8. Left panel: horizontal resolution of N₂O VMRs when retrieved from UTLS-1 observations using the natural retrieval grid. Right panel: values of the horizontal resolution at 18 km extracted from the map in the left panel (green line) and values, at the same altitude, when the 2.25 deg separation is used for the horizontal grid (red line).

[Title Page](#)[Abstract](#)[Introduction](#)[Conclusions](#)[References](#)[Tables](#)[Figures](#)[⏪](#)[⏩](#)[◀](#)[▶](#)[Back](#)[Close](#)[Full Screen / Esc](#)[Printer-friendly Version](#)[Interactive Discussion](#)

Two-dimensional performance of MIPAS observation modes

M. Carlotti et al.

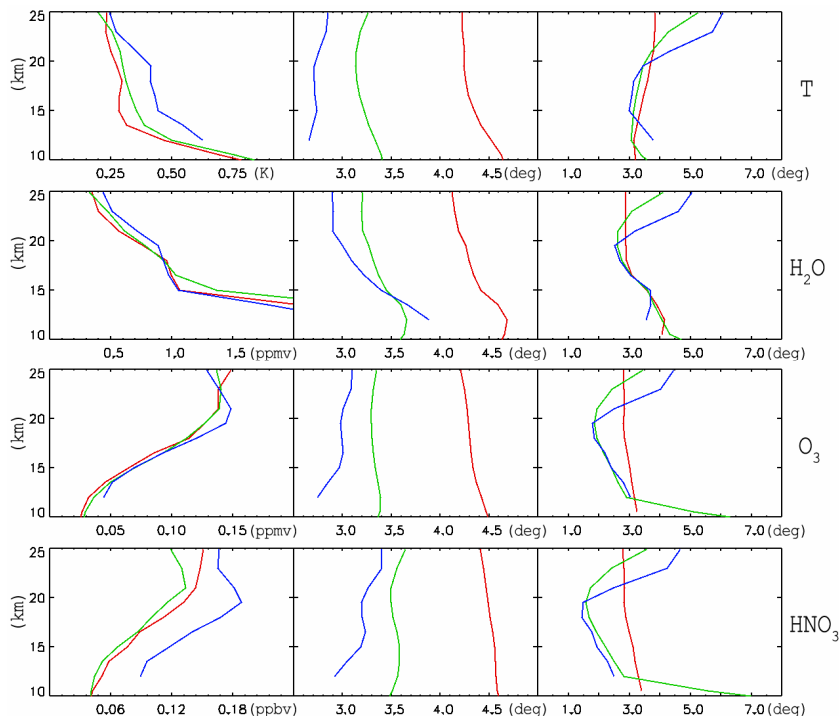
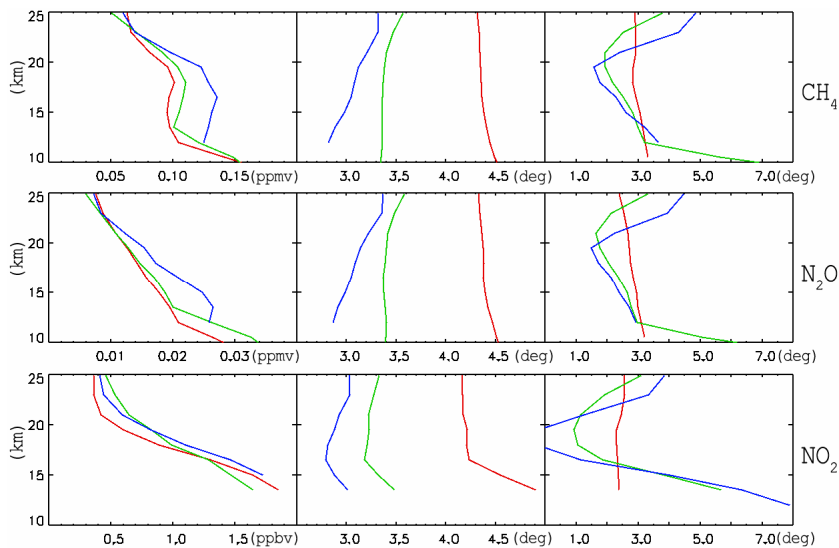


Fig. 9. Standard deviation of the difference between retrieved and the reference profiles (left column), average horizontal resolution (middle column) and average vertical resolution (right column) for NOM (red), UTLS-1 (green) and UTLS-2 (blue). NOM and UTLS-1 plots refer to their natural retrieval grids, UTLS-2 plots refer to the 2.25 deg retrieval grid.

[Title Page](#)
[Abstract](#)
[Introduction](#)
[Conclusions](#)
[References](#)
[Tables](#)
[Figures](#)
[◀](#)
[▶](#)
[◀](#)
[▶](#)
[Back](#)
[Close](#)
[Full Screen / Esc](#)
[Printer-friendly Version](#)
[Interactive Discussion](#)

Two-dimensional performance of MIPAS observation modes

M. Carlotti et al.

**Fig. 9.** Continued.